Materials Transactions, Vol. 43, No. 11 (2002) pp. 2808 to 2812

Effects of TiC and $Cr_{23}C_6$ Carbides on Creep-Fatigue Properties in AISI 321 Stainless Steel

Kyung Seon Min[1, *1], Soo Chan Lee[2] and Soo Woo Nam[1, *2]

[1]*Department of Materials Science and Engineering, Korea Advanced Institute of Science and Technology, 373-1 Guseong-dong, Yuseong-gu, Daejeon, 305-701, Korea*
[2]*POSCO Technical Research Laboratory, #1 Koedong-dong, Nam-ku, Pohang, 790-785, Korea*

In order to investigate the effects of TiC and $Cr_{23}C_6$ carbides on creep-fatigue behaviors, total strain range controlled creep-fatigue tests of TiC and $Cr_{23}C_6$ aged AISI 321 stainless steels with the same carbide density at the grain boundary were conducted at 600°C. It is observed that creep-fatigue life of TiC aged alloy is longer than that of $Cr_{23}C_6$ aged alloy in the same test conditions. To verify the origin of the difference in creep-fatigue life between the two alloys, microstructural observations are conducted by scanning electron microscope (SEM) and transmission electron microscope (TEM). It is understood to be due to the strong cavitation resistance of TiC aged alloy compared with that of $Cr_{23}C_6$ aged alloy. It is considered that formation and growth of cavities are retarded by strong interfacial affinity between TiC and matrix.

(Received June 21, 2002; Accepted September 2, 2002)

Keywords: *American Iron and Steel Institute (AISI) 321 stainless steel, titanium carbide, creep-fatigue interaction, grain boundary cavitation*

1. Introduction

It is well known that AISI 321 stainless steels with a higher composition of Ti than other AISI 304 stainless steels and, consequently, have good corrosion resistance as they inhibited grain boundary sensitization.[1–3] For this reason, AISI 321 stainless steels are used in core components of breeder reactors, high pressure pipes, heat exchangers in chemical plants and engine turbines in automobiles and aircrafts.

The TiC carbides that are precipitated in austenitic stainless steels satisfy two purposes: First, their precipitation limits the formation of chromium-rich $M_{23}C_6$ type carbide at grain boundary and prevents intergranular stress corrosion. Second, if TiC carbides are presented as a fine dispersion in matrices and grain boundaries, they improve tensile and creep strength significantly at both high and low temperatures.[4–9]

Generally, the carbide at grain boundaries provides the preferential site for the cavity nucleation under creep-fatigue interaction conditions.[10–16] The higher the carbide density at grain boundaries, the shorter creep-fatigue life of materials.[13,16] Therefore, it is known that the control of carbide density is an important factor in determining the creep-fatigue life. When Ti is added to austenitic stainless steels, TiC precipitates are observed to be uniformly formed in the grain and grain boundary. In particular, cavitation could be affected by TiC carbides at the grain boundary during the high temperature fatigue cycle. Although many researchers have investigated Ti-modified stainless steels, most studies of TiC aged 321 stainless steels have been conducted from the viewpoint of corrosion resistances. However, there are few reports that consider the mechanical effects of TiC on the low cycle fatigue interaction.[9,17]

In the present study, total strain range controlled creep-fatigue tests with AISI 321 stainless steel have been conducted in order to investigate the difference in creep-fatigue resistance of TiC and $Cr_{23}C_6$ carbides in AISI 321 stainless steel with the same carbide density at the grain boundary.

2. Experimental Procedure

Creep-fatigue tests were carried out with AISI 321 stainless steel whose chemical composition and heat treatment conditions before fatigue testing are shown in Table 1. After solution heat treatments, two different aging treatment conditions were designed and the steel was aged to form TiC and $Cr_{23}C_6$ carbides, separately. For $Cr_{23}C_6$ carbide precipitation heat treatment of (1) process is applied and for TiC carbide (2) process is conducted. When TiC and $Cr_{23}C_6$ have the same size and density at the grain boundary, different lattice parameters of the carbides could affect mechanical properties of the alloys. After solid solution treatment for TiC carbide precipitation, the alloy was furnace-cooled to obtain the similar size and density of TiC at grain boundaries compared with those of $Cr_{23}C_6$ obtained by the (1) process.

Total strain controlled low cycle fatigue tests with 30 minute tensile hold time at the maximum tensile strain were conducted at 600°C. The tested total strain ranges ($\Delta\varepsilon_t$) were $\pm$1.0, $\pm$1.5 and $\pm$2.0%. The number of cycles to failure, N_{cr} was defined as the number of cycles leading to a 20% reduction in a saturated tensile peak load.

In order to observe grain boundary carbides and cavities, specimens were chilled in liquid nitrogen (LNT) to be broken by impact along the most damaged and weakest part and, then, examined with a scanning electron microscope (SEM) Jeol 840A. The morphologies of carbides were observed by a transmission electron microscope (TEM) Philips Technai F20 operated at 300 kV. TEM foils were prepared by the twin-jet method using 5 vol% perchloric acid + 95 vol% acetic acid at 15°C, 30 V.

*1Graduate Student, Korea Advanced Institute of Science and Technology.
*2Jointly Appointed at the Center for the Advanced Aerospace Materials.

Table 1 The chemical composition and the heat treatment schedules for AISI 321 stainless steel.

(all in mass%)

C	Ti	Si	Mn	P	S	Cr	Ni	Mo	Cu	N
0.03	0.257	0.602	1.44	0.024	0.002	17.90	9.15	0.096	0.198	0.012

Aging heat treatments for either $Cr_{23}C_6$ or TiC after solution treatment

(1) $Cr_{23}C_6$ aged: Solution treatment (1100°C/0.5 h/WQ) → Aging treatment (750°C/24 h/WQ)

(2) TiC aged: Solution treatment (1100°C/0.5 h) → Furnace cooled to 930°C → Aging treatment (930°C/10 h/WQ)

Table 2 The tensile properties for TiC and $Cr_{23}C_6$ aged AISI 321 stainless steel at 600°C.

	Yield strength (MPa)	Ultimate tensile strength (MPa)	Elongation (%)
TiC aged 321	178.0	335.6	34.4
$Cr_{23}C_6$ aged 321	160.3	337.4	34.4

3. Results and Discussions

3.1 Microstructure before test

After the aging heat treatment, grain sizes of TiC and $Cr_{23}C_6$ aged 321 stainless steels are observed to be similar to 100 μm shown in Figs. 1(a) and (b), respectively.

TiC and $Cr_{23}C_6$ carbide densities on grain boundaries in the two alloys also have similar values (TiC: $1.11 \times 10^5\,m^{-1}$, $Cr_{23}C_6$: $1.18 \times 10^5\,m^{-1}$) and the shape of carbides is found to be similar as shown in Figs. 1(c) and (d), respectively. It is reported that creep-fatigue properties are affected by the carbide density on the grain boundary, carbide morphology and interfacial energy between carbides and matrix of neighboring grains.[13,14] Because of the fact that the fatigue lives of the two alloys are different even though they have similar carbide density and shape as shown in Fig. 1, it is suggested that creep-fatigue lives of the two alloys may be affected by the other factors rather than by carbide density and shape.

3.2 Tensile properties

Mechanical properties of TiC and $Cr_{23}C_6$ aged alloys are tabulated in Table 2. It is observed that the two alloys have similar ultimate tensile strength and elongation, but differ in the yield strength. In Table 2, the yield strength of TiC aged alloy is higher than that of $Cr_{23}C_6$ aged alloy. This is considered to be because many TiC particles in the grain prevent dislocations to move freely. This result implies that the ultimate tensile strength is not affected by different kinds of carbides in grain boundary.

3.3 Creep-fatigue properties

The results of the creep-fatigue tests are plotted in Fig. 2 in terms of the plastic strain range with the critical number of cycles (N_{cr}). The plot indicates that the creep-fatigue life of TiC aged alloy is 40% longer than that of $Cr_{23}C_6$ aged alloy at the same total strain range. As previously mentioned, when the austenitic stainless steel was tested under the creep-fatigue interaction condition, the material failed due to the accumulation of the critical amount of the grain boundary cavitation damage.[10–16] It is also well known that carbide density and morphology could seriously affect the grain boundary cavitation of austenitic stainless steels.[13,14] However, creep-fatigue lives between the two tested alloys show remarkable difference in spite of the similar carbide density and morphology. In the next section, microstructural observation is undertaken to understand how TiC or $Cr_{23}C_6$ carbides affect the creep-fatigue life.

3.4 Microstructural analysis

Figure 3 and 4 show fractured surfaces of TiC and $Cr_{23}C_6$ aged alloys that were fractured by impact at the liquid nitrogen temperature (LNT) after a creep-fatigue test at 600°C with $\Delta\varepsilon_t$ of ±1.0% and 30 minute tensile hold. Figures 3(a) and (b) show the crack propagation regions and fractured surfaces by impact at the LNT of TiC aged alloy, respectively. Intergranular fracture modes are shown at both surfaces along the grain boundary, but the cavities and small dimples are observed in each fractured grain boundary as shown in Fig. 3(b). Figure 3(c) is a higher magnification of Fig. 3(b). From this observation, it is clearly observed that the cavities and dimples are co-existing in TiC aged alloy during the creep-fatigue interaction.

Figure 4 shows fractured surfaces of $Cr_{23}C_6$ aged alloy after a creep-fatigue test. From the observation of Figs. 4(a) and (b), the intergranular fracture mode of $Cr_{23}C_6$ aged alloy is clearer and better developed compared to that of TiC aged alloy. Also, Fig. 4(c) is a higher magnification of the fractured surface by impact at LNT as shown in Fig. 3(c). Figure 4(c) shows the fractured grain boundary with cavities formed during the creep-fatigue loading at the $Cr_{23}C_6$ carbides. A few secondary cracks along the grain boundaries are observed in Fig. 4(a), and the facets are flat in Fig. 4(b). On the other hand, the intergranular fracture mode in Fig. 3(a) is not so clear as Fig. 4(a), and the facets are covered with many small dimples in Fig. 3(b). It means that the fracture mode of TiC aged alloy is more ductile than that of $Cr_{23}C_6$ aged alloy during the creep-fatigue interaction. In Fig. 4(c), the many small cavities are formed during the creep-fatigue test and are appeared on the brittle flat facets after the impact at LNT. In Fig. 3(c), distinct dimples are formed all over the facets of fractured surfaces by impact at LNT because less cavities and the grain boundary is more ductile. From the difference in fracture modes between TiC and $Cr_{23}C_6$ aged alloys, it is expected that cavitation resistance between the two alloys is different with the different carbides. It is verified from the previous reports[12–14] that grain boundary cavities are continuously formed and grown with fatigue cycles under creep-fatigue interaction condition. It is also generally known that cavities are nucleated at geometrical irregularities on grain boundaries where high tensile stress concentration can be developed.

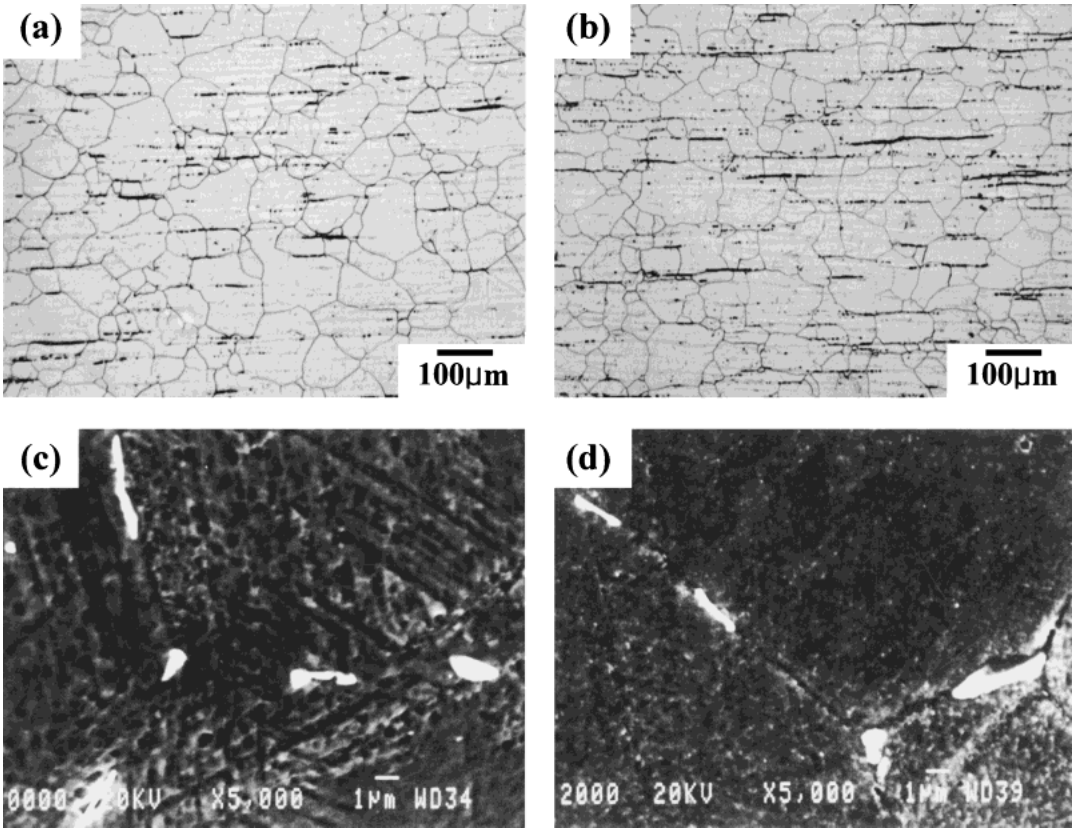

Fig. 1 Micrographs showing grain size and grain boundary carbides for TiC and $Cr_{23}C_6$ aged AISI 321 stainless steels (a) OM for TiC aged alloy, (b) OM for $Cr_{23}C_6$ aged alloy, (c) SEM for TiC aged alloy, (d) SEM for $Cr_{23}C_6$ aged alloy.

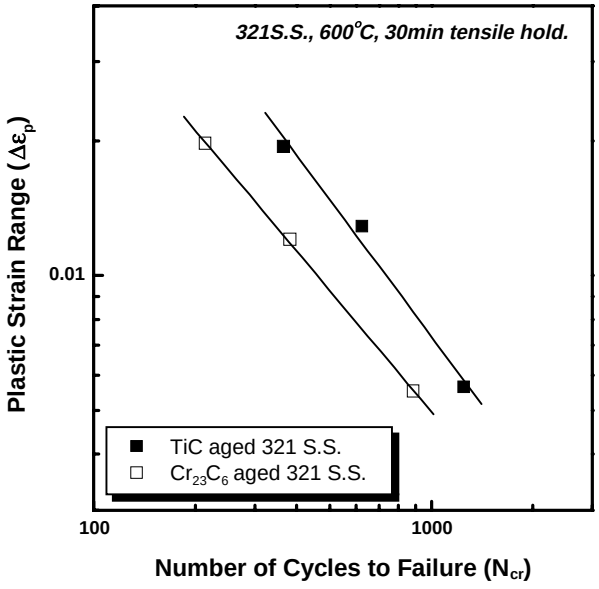

Fig. 2 Relationship between plastic strain range and the critical number of cycles for TiC and $Cr_{23}C_6$ aged AISI 321 stainless steel.

In spite of the same carbide density and shape between two alloys, the degree of grain boundary cavitation is different between TiC and $Cr_{23}C_6$ aged alloys. This implies that cavitation resistance of TiC aged alloy is stronger than that of $Cr_{23}C_6$ aged alloy. This observation is well matched to the test results of creep-fatigue interaction.

From this observation, it is considered that cavitation behaviors may be affected by interfacial interactions between grain boundary carbides and neighboring grains near carbides. It is expected that strong interfacial affinity between carbides and matrices prevents the formation and growth of cavities.

Figure 5 shows the dislocation structure of TiC and $Cr_{23}C_6$ aged alloys after a creep-fatigue test at 600°C with $\Delta\varepsilon_t$ of $\pm$1.5% and 30 minute tensile hold. The dislocation structure of two alloys shows cell structures. It is reported that planar or band-like dislocation arrangements are found in low temperature fatigued materials with low stacking fault energy such as austenitic stainless steels and that cell structures of dislocations are formed by cross-slip and climb at the elevated temperature.[18,19]

Cell structure of TiC aged alloy is less developed than that of $Cr_{23}C_6$ aged alloy in Fig. 5. It is suggested that this difference of dislocation structure is caused by small TiC particles in the matrix. Despite fully aging heat treatments conducted to obtain the same carbide density of TiC at the grain boundary and $Cr_{23}C_6$ carbide, many small TiC carbides are precipitated in the matrix of AISI 321 stainless steel. Because the dislocation movement is retarded by these TiC carbides, the dislocation structure of TiC aged alloy with precipitates in the matrix is less developed than that of $Cr_{23}C_6$ aged alloy without precipitates in the matrix. This present result suggests that the resistance against the grain boundary cavitation during creep-fatigue deformation of TiC aged alloy is higher than that of $Cr_{23}C_6$ aged alloy.

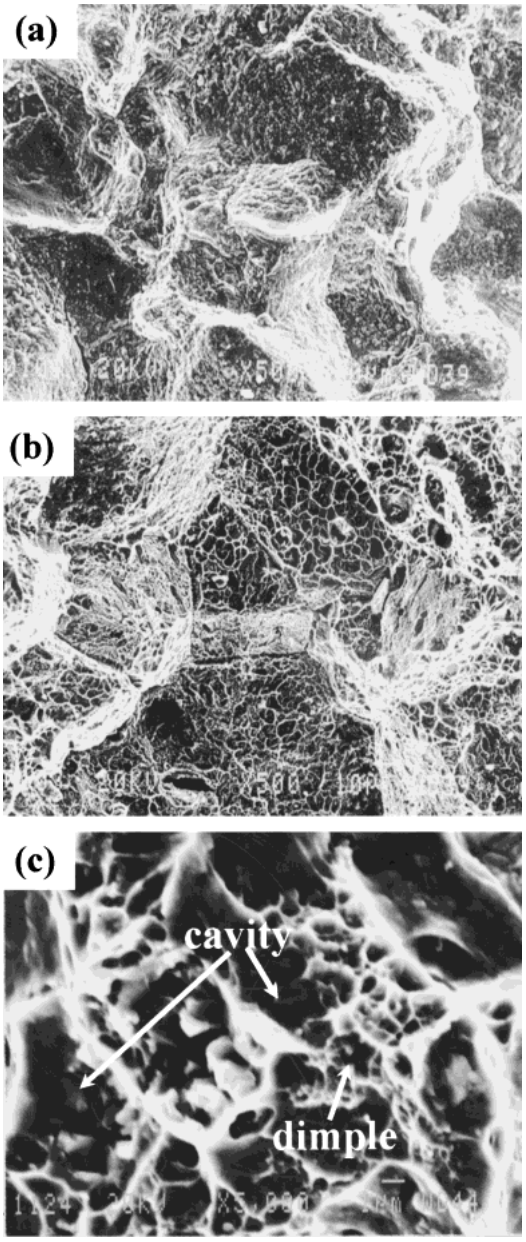

Fig. 3 SEM micrographs showing the fractured surfaces of TiC aged AISI 321 stainless steel after creep-fatigue test ($T = 600°C$, $\Delta\varepsilon_t = \pm 1.0\%$, $t_h = 30$ min) (a) crack propagated surface, (b) fractured surface by impact at LNT, (c) high magnification of (b).

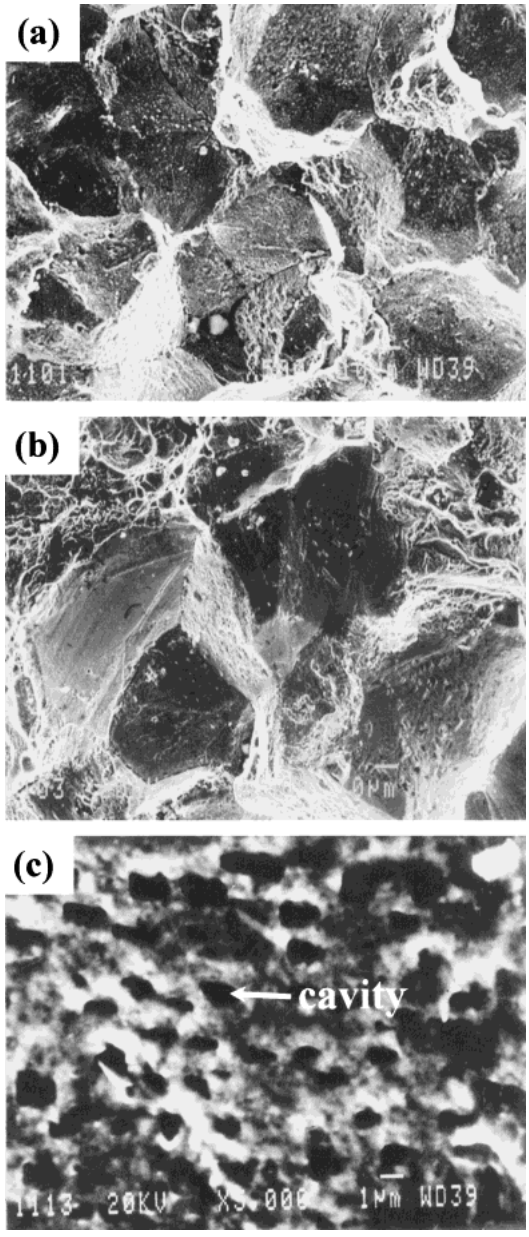

Fig. 4 SEM micrographs showing the fractured surfaces of $Cr_{23}C_6$ aged AISI 321 stainless steel after creep-fatigue test ($T = 600°C$, $\Delta\varepsilon_t = \pm 1.0\%$, $t_h = 30$ min) (a) crack propagated surface, (b) fractured surface by impact at LNT, (c) high magnification of (b).

4. Conclusions

Total strain range controlled creep-fatigue tests of TiC and $Cr_{23}C_6$ aged 321 stainless steels with the same grain carbide density were conducted at 600°C in order to investigate effects of TiC and $Cr_{23}C_6$ carbides on the creep-fatigue properties.

(1) It is observed that creep-fatigue life of TiC aged alloy is longer than that of $Cr_{23}C_6$ aged alloy.

(2) The difference of creep-fatigue life between the two alloys is based on the strong cavitation resistance of TiC aged alloy compared with that of $Cr_{23}C_6$ aged alloy. From microstructural observation, it is verified that formation and growth of cavities in TiC aged alloy are more retarded than those in $Cr_{23}C_6$ aged alloy.

Acknowledgments

This research was sponsored by POSCO as a project of BK21 (Brain Korea 21). The authors would like to express their appreciation for the financial support.

REFERENCES

1) J. H. Payer and R. W. Staehle: Corrosion **31** (1975) 30–36.
2) C. Hoffmann and A. J. Mcevily: Metall. Trans. A **13** (1982) 923–927.
3) M. Schwind, J. Källqvist, J.-O. Nilsson, J. Ågren and H.-O. Andrén: Acta Mater. **48** (2000) 2473–2481.
4) T. Thorvaldsson and G. L. Dunlop: Met. Sci. (1980) 513–518.
5) A. S. Grot and J. E. Spruiell: Metall. Trans. A **6** (1975) 2023–2030.
6) J. M. Leitnaker and J. Bentley: Metall. Trans. A **8** (1977) 1605–1613.
7) J. K. L. Lai: Mater. Sci. Tech. **1** (1985) 97–100.
8) B. A. Senior: Mater. Sci. Eng. **100** (1988) 219–227.
9) O. R. Arzate and L. Martinez: Mater. Sci. Eng. A **101** (1988) 1–6.

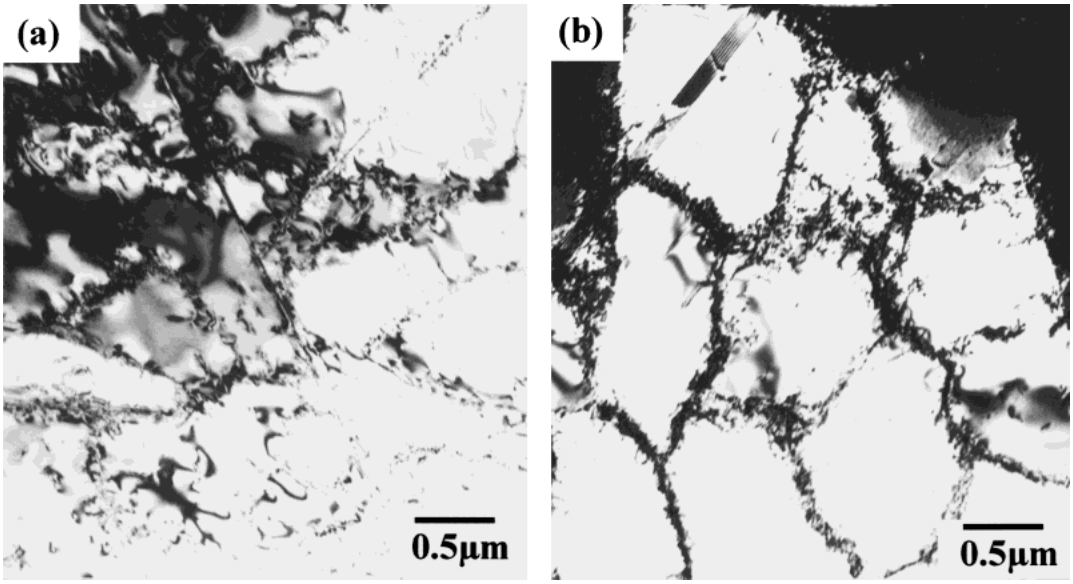

Fig. 5 TEM micrographs showing the dislocation structures of TiC and $Cr_{23}C_6$ aged AISI 321 stainless steels after creep-fatigue test ($T = 600°C$, $\Delta\varepsilon_t = \pm 1.5\%$, $t_h = 30$ min) (a) dislocation structure of TiC aged alloy, (b) dislocation structure of $Cr_{23}C_6$ aged alloy.

10) P. S. Maiya and S. Majumdar: Metall. Trans. A **8** (1977) 1651–1660.
11) M. H. Yoo and H. Trinkaus: Metall. Trans. A **14** (1983) 547–561.
12) J. W. Hong, S. W. Nam and K.-T. Rie: J. Mater. Sci. **20** (1985) 3763–3779.
13) B. G. Choi, S. W. Nam, Y. C. Yoon and J. J. Kim: J. Mater. Sci. **31** (1996) 4957–4966.
14) S. W. Nam, Y. C. Yoon, B. G. Choi, J. M. Lee and J. W. Hong: Metall. Mater. Trans. A **27** (1996) 1273–1281.
15) J. M. Lee and S. W. Nam: Int. J. Damage. Mech. **2** (1993) 4–15.
16) S. W. Nam: Mater. Sci. Eng. **322** (2002) 64–72.
17) K. Yamaguchi and K. Kanazawa: Metall. Trans. A **10** (1979) 1445–1451.
18) H. Nahm, J. Moteff and D. R. Diercks: Acta Metall. **25** (1977) 107–116.
19) A. M. Ermi and J. Moteff: Metall. Trans. A **13** (1982) 1577–1588.